

Superconductivity and physical properties of a LaRhSn single crystal

Matúš Mihalik^a, Vladimír Sechovský^{a,*}, Martin Diviš^a,
Slavomír Gabáni^b, Marián Mihalik^b

^a Charles University, Faculty of Mathematics and Physics, Department of Condensed Matter Physics,
Ke Karlovu 5, 121 16 Prague 2, Czech Republic

^b Slovak Academy of Sciences, Institute of Experimental Physics, Watsonova 47, 04001 Košice, Slovakia

Received 10 December 2006; received in revised form 22 January 2007; accepted 23 January 2007

Available online 28 January 2007

Abstract

Single crystals of LaRhSn have been grown and studied with respect to the electrical resistivity and specific heat, which were measured in the temperature range from 0.1 to 300 K in various magnetic fields. The compound was found to be superconducting at temperatures lower than $T_c = 1.85 \pm 0.05$ K. The critical field B_{c2} and also the temperature dependence $B_{c2}(T)$ were found to be dependent on the geometry of the experiment with respect to the direction of the magnetic field (applied along the *a*- or *c*-axis). The electrical resistivity measurements at temperatures higher than 2 K revealed metallic behavior with a considerable anisotropy between the *a*-axis and the *c*-axis. The experimental results are also discussed in the light of our *ab initio* electronic-structure calculations.

© 2007 Elsevier B.V. All rights reserved.

PACS: 74.70.Dd; 74.25.Fy; 74.25.Bt; 71.15.Mb

Keywords: Intermetallics; Superconductors; Heat capacity; Electrical resistivity

1. Introduction

In recent years, there has been a great deal of interest in the study of rare-earth containing intermetallic compounds of the type RTX, where R is a rare-earth element, T and X is a d- and a p-metal, respectively. These compounds crystallize in a variety of structure types, depending on the T and X element species and exhibit various interesting physical properties. The most attractive are superconductivity with the critical temperature around 2 K (LaRhSn [1] and LaRhSb [2]), Kondo behavior (CeNiSn [3] and CeRhSb [4]) and non-Fermi-liquid behavior (CeRhSn [5]). Numerous Sn-containing compounds exhibit antiferromagnetic ordering of rare-earth magnetic moments (NdNiSn [6], CePdSn [7] and other compounds) whereas many compounds with Sb order ferromagnetically (for example NdNiSb [8], PrPdSb [9]).

LaRhSn crystallizes in the hexagonal ZrNiAl-type structure (space group $P\bar{6}2m$). First, electrical resistivity and ac suscepti-

bility measurements on polycrystalline LaRhSn sample revealed superconducting phase with the critical temperature $T_c = 1.7$ K [10]. Next Ho et al. studied also polycrystalline samples and reported $T_c = 2$ K and the critical field for destroying superconductivity rising from 0.1 T at 1.6 K to 0.7 T at 0.2 K [1]. It is worth to note that the magnetic susceptibility of LaRhSn in the normal state is remarkably higher than the susceptibility of CeRhSn [11]. Up to now a LaRhSn single crystal was studied only as a nonmagnetic analogue within investigation of the CeRhSn compound [5]. Since the superconducting transition in LaRhSn was studied so far only on polycrystalline samples [1] we decided to grow a single crystal and to study the specific heat and electrical resistivity near the critical temperature T_c . To understand the behavior of LaRhSn more closely we performed also *ab initio* calculations of electronic structure of this compound and discuss the results of calculations together with experimental data.

2. Experimental and calculation details

Two single crystals (i) and (ii) of LaRhSn have been grown by a modified Czochralski method in a tri-arc furnace under purified Ar atmosphere from a melt

* Corresponding author.

E-mail address: sech@mag.mff.cuni.cz (V. Sechovský).

consisting of the stoichiometric composition of the high purity (La: 99.9%; Rh: 99.9; Sn: 99.8) element metals using a tungsten rod as a seed. The quality of the crystals was checked and confirmed by Laue patterns. Rietveld analysis of the X-ray powder diffractogram revealed only the LaRhSn phase within the sensitivity of the method. The lattice parameters of both single crystals were found identical ($a = 0.7479(3)$ nm; $c = 0.4217(4)$ nm; $x_{\text{La}} = 0.591(4)$ and $x_{\text{Sn}} = 0.243(8)$) and are in good agreement with data published by Slebarski et al. [11].

Temperature dependences of the specific heat (C) and electrical resistivity (ρ) were measured with the PPMS (Quantum Design) apparatus using a ^3He insert for cooling below 2 K. We used the crystal (ii) for these measurements. The electrical resistivity was measured by a standard four-probe ac method with driving current of 500 μA . The experimental error for measuring the voltage on the sample was less than 4%. The temperature of superconducting transition T_c in all experiments (with and without magnetic field) was determined with the temperature at which the resistivity drops to zero.

The specific heat was measured by the relaxation method described in Ref. [12] with the error less than 3% for temperatures lower than 2 K (He3 insert) and less than 1% for $T > 2$ K.

The critical field (B_{c2}) was studied on both the crystals (i) and (ii) in the Oxford TLE-200 $^3\text{He}^4\text{He}$ dilution refrigerator and was determined as a field in which the maximum slope of the $\rho(B)$ dependence at constant temperature was observed. Temperature was measured by a calibrated germanium Lake Shore sensor GR-200A-50. In this experiment the driving current was 100 μA .

The electronic structure was calculated in the framework of the density functional theory (DFT). We have used both the local density approximation (LDA) [13] and the generalized gradient approximation (GGA) [14]. The Kohn–Sham equations of DFT were solved using full potential augmented plane wave plus local orbitals (APW + lo) WIEN2k code [15]. The relativistic effects were treated in the scalar relativistic approximation [16]. Atomic sphere (AS) radii of 2.5, 2.3 and 2.1 Bohr radii (1 Bohr = 52.9177 pm) were chosen for La, Rh and Sn, respectively. We have used a basis of about 1450 APW functions (about 160 per atom) in the interstitial region and the maximum $l = 12$ in the expansion of the radial wave functions inside the AS to represent the valence states. Local orbitals were used to treat the fully occupied La-5s-5p, Rh-4s-4p and Sn-4p-4d states with the valence states in a single energy window. The advantage of this treatment is that the above-mentioned semicore states are orthogonal to the valence states. Both the potential and the charge density were expanded inside the AS into crystal harmonics up to $L = 6$ and in the interstitial region into a Fourier series with about 5793 K stars. For the Brillouin zone (BZ) integration, a modified tetrahedron method [15] with 198 special k -points in the irreducible wedge (2000 k -points in the full BZ) was used to construct the charge density in each self-consistency step. We have carefully checked that with these parameters the calculations converge. The values of the internal structure parameters x_{La} and x_{Sn} were obtained by minimizing the forces for fixed values a and c determined from experiment. Such calculated values of the free internal parameters are close to the values determined from the experiment.

We also wanted to compare the performance of LDA and GGA with respect to the equilibrium volume of LaRhSn. The experimental ca ratio and the symmetry-free structure parameters obtained from minimization of the forces were used and kept constant during the calculations. The LDA value of the equilibrium volume is smaller comparing the experimental value by about 4.6%. This is a typical deviation usually obtained in LDA calculations. The GGA, on the other hand, overestimated experimental V_0 by only 2.3%, so the GGA provides a better equilibrium volume than LDA.

3. Results

The specific heat of LaRhSn (Fig. 1.) exhibits a lambda anomaly and reaches the maximum value $C_s = 0.0485 \text{ J mol}^{-1} \text{ K}^{-1}$ at $T_c = 1.85 \pm 0.05$ K. Taking into resistivity data discussed below we attributed the $C(T)$ peak to the transition from the normal to the superconducting state. When a magnetic field is applied along the c -axis the $C(T)$ anomaly moves to lower temperatures and becomes reduced. Finally, in the field of 0.3 T field the peak is no more indicated in the temperature

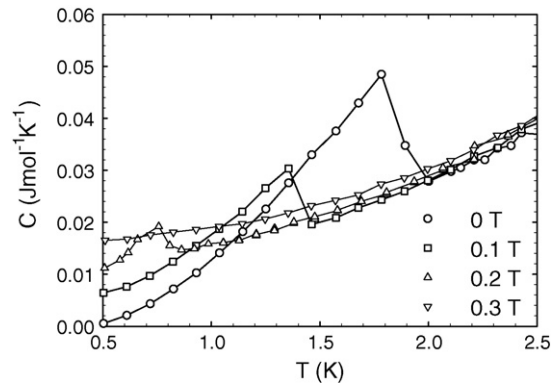


Fig. 1. A low temperature detail of the temperature dependence of the specific heat of the crystal (ii) of LaRhSn, which shows evolution of the superconducting transition with respect to the magnetic field applied along the c -axis. The lines are only guides for the eye.

range (0.5–300 K) of our measurement on PPMS. At $T_c = 1.85$ (zero-field value) the sample in the field of 0.1 T is still in the normal state and the specific heat amounts only the value $C_n = 0.0243 \text{ J mol}^{-1} \text{ K}^{-1}$. Then the ratio $(C_s - C_n)/C_n \cong 1$ is much lower than the value of 1.43 predicted by BCS theory.

In the temperature range 2–8 K the specific heat data fit with the equation $C = \gamma T + \beta T^3$, where γT and βT^3 describe the electronic and phonon contributions to the specific heat, respectively, with the parameters $\gamma = 10.9 \text{ mJ mol}^{-1} \text{ K}^{-2}$ and $\beta = 6.2 \times 10^{-4} \text{ J mol}^{-1} \text{ K}^{-4}$. From our first principles band structure calculations based on the density functional theory we have obtained $\gamma_{\text{DFT}} = 6.68 \text{ mJ mol}^{-1} \text{ K}^{-2}$ by the GGA method. The calculated Fermi level is situated at a peak in the density of states (DOS) (see Fig. 2). The DOS at Fermi level leads to enhancement factor $\lambda = 0.63$ with λ defined by $\gamma = \gamma_{\text{DFT}} (1 + \lambda)$.

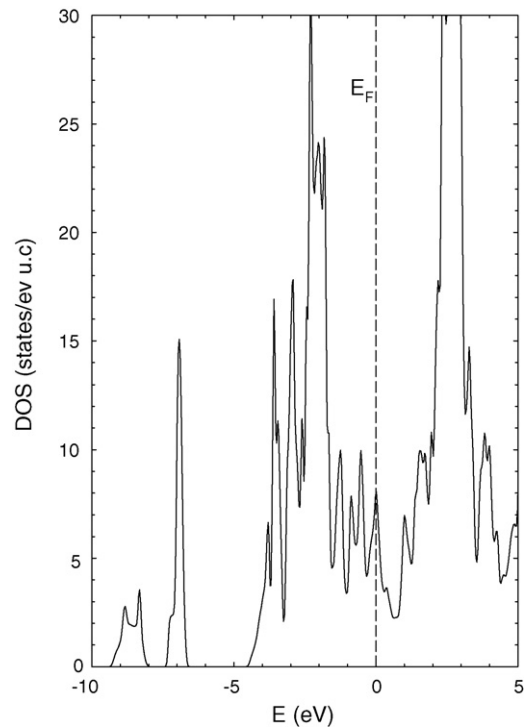


Fig. 2. The density of states curve calculated for the LaRhSn compound.

Download English Version:

<https://daneshyari.com/en/article/1624690>

Download Persian Version:

<https://daneshyari.com/article/1624690>

[Daneshyari.com](https://daneshyari.com)